J Mater Sci (2006) 41:5433–5440
DOI 10.1007/s10853-006-0290-6

On promoting dispersion and intercalation of bentonite in high density polyethylene by grafting vinyl triethoxysilane

Zhengping Fang · Yuzhen Xu · Lifang Tong

Received: 5 July 2005 / Accepted: 12 October 2005 / Published online: 13 June 2006

Abstract Vinyl triethoxysilane grafted high density polyethylene (HDPE-g-YDH151)/Bentonite (BT) composites were prepared via melt compounding and compared with HDPE/BT composites. FTIR proved that HDPE-g-YDH151 is chemically bonded to BT sheets. XRD, SEM and TEM results indicated that the introduction of YDH151 promoted the dispersion and intercalation of BT into HDPE. Consequently, HDPE-g-YDH151/BT composites show satisfied mechanical properties, e.g., the composite with 2phr BT has an elongation at break 29% higher and Young's modulus 32% higher than that of HDPE-g-YDH151.Comparatively, BT aggregated in HDPE/BT composites and all the mechanical properties decreased. Because of high interfacial adhesion between HDPE-g-YDH151 matrix and exfoliated BT, which reduces the mobility of crystallizable PE chain segments, and subsequently reduces the crystallization ability. In comparison, the addition of BT to HDPE did not affect the crystallization behavior of the later.

Introduction

Polymer-layered silicate (PLS) nanocomposites have attracted great attention due to their academic and industrial importance. They have shown dramatic improvements in mechanical, thermal, and barrier properties with a small amount of inorganic layered silicate [1–9]. Moreover, they can provide good model system for the studies of the phase behavior of polymer-nanoparticle mixtures [10–21] as well as polymer chain dynamics in the confined geometry [22–29].

Polyethylene is one of the most widely used polyolefin. Since it does not contain any polar group in its backbone, the homogeneous dispersion and exfoliation of the clay minerals in polyethylene is not realized even when the clay is organically modified [30–32]. Jeon et al. [31] reported the intercalated morphology of high-density polyethylene (HDPE) nanocomposites prepared by solution-blending of HDPE with sodium montmorillonite cation exchanged with protonated dodecylamine. However, the presence of fairly large stacks indicated poor dispersion. Only when in situ polymerization was performed polyethylene/silicate showed an exfoliated morphology [33–35].

Initial attempts to create the non-polar polymer/silicate nanocomposites by melt intercalation were based on the introduction of a modified oligomer to mediate the polarity between the silicate surface and polymer [36–44]. One of the typical examples is the polypropylene/silicate nanocomposite system by Toyota. They used polypropylene oligomer modified with about 10 wt% of maleic anhydride (MA) as a compatibilizer and silicate exchanged with stearylammonium cation to obtain exfoliated or semiexfoliated silicate morphology [38, 39, 42–44]. In such a nanocomposite system, the miscibility between maleated oligomer and matrix polymer played a key role in determining the composite properties.

Although intensive research efforts have been devoted to the development of novel synthetic approaches in polymer nanocomposites as well as to the investigation of the physical properties of these materials in recent years, there

Z. Fang (✉) · Y. Xu · L. Tong
Institute of Polymer Composites, Zhejiang University, Hangzhou 310027, P. R. China
e-mail: zpfang@zju.edu.cn

is a great need to define the exact role of nanofiller particles in the matrix and the effect of interfacial interactions between the silicate nanolayers and the polymer matrix during the deformation process.

In this work, we choose vinyl triethoxysilane (YDH151) as grafting monomer to graft HDPE. YDH151 is a good polar monomer and it has been widely used to graft polyethylene to induce polar groups in PE chains. Furthermore the hydroxyl of YDH151 hydrolysate can react with the amidogens of BT, and it is not acidic and non-poisonous. So using YDH-151 as grafting monomer can avoid the possible corrosion and poison induced by using MA. The reactions between the hydroxyl of YDH151 and the amidogens of BT were studied. The structure and properties of HDPE-g-YDH151/BT composites were also investigated and compared with HDPE/BT system.

Experimental

Materials

The modified bentonite (BT) (C18-BT) was supplied by Zhejiang Huate Clay Products of China, which was ion-exchanged with octadyl trimethyl ammonium. HDPE (5502#, MFR = 0.35 g/10 min) was from Daelim Corporation, Korea. Vinyl triethoxysilane(YDH151) and dicumyl peroxide (DCP) were used as the grafting monomer and a radical initiator of high density polyethylene, respectively. All chemicals were used as received.

Preparation of composites

All composites were prepared via melt compounding at 160 °C in ThermoHaake Rheomix with a screw speed of 60 rpm, and the mixing time was 20 min for each sample. The mixed samples were transferred to a mold and preheated at 160 °C for 3 min, then pressed at 14 MPa, and successively cooled to room temperature while maintaining the pressure to obtain the composite sheets for further measurements.

Characterization

FT-IR analysis

The FT-IR spectra were recorded on a Vector-22 FT-IR spectrometer. The samples were dissolved in xylene at a concentration of 2 wt.% and precipitated by chloroform, then filtered and dried in a vacuum oven at 80 °C for 24 h. At last, the purified samples were pressed to obtain membranes whose thickness were about 40–60 μm.

X-ray diffraction

X-ray diffraction (XRD) was used to examine the dispersion of BT in composites. XRD was carried out by using a Rigaku X-ray generator (Cu Kα radiation with λ = 1.54 Å) at room temperature. The diffractograms were obtained at the scattering angles from 2° to 12°, at a scanning rate of 4°/min.

Transmission electron microscopy

The transmission electron micrographs were obtained with a JEM-1200EX electron microscope to examine the dispersion and exfoliation status of BT in composites. The nanocomposite samples for TEM observation were ultra-thin-sectioned using a microtome equipped with a diamond knife. The sections (100–200 nm in thickness) were cut from a piece of about 1×1 mm^2, and they were collected in a trough filled with water and placed on 200 mesh copper grid.

Scanning electron microscopy

The side surface of the tensile specimens near the fracture site was inspected in a HITACHI S-570 scanning electron microscope (SEM). The surfaces were coated with a thin layer of gold to avoid electrostatic charging during examination.

Differential scanning calorimetry

Thermal properties of composites were measured with a Perkin-Elmer 7 differential scanning calorimeter (DSC). The temperature was raised from 40 to 180 °C at a heating rate of 40 °C/min, and after a period of 3 min it was swept back at –10 °C/min. Finally a heating scanning from 40 to 180 °C (at 10 °C/min) was carried out.

Tensile testing

Tensile properties of composite were measured using an RG2000-10 Universal Tensile Tester according to ASTM D-638 standard. Five samples of each batch were measured. The samples were performed with a 50 mm/min extension rate at room temperature.

Extraction and characterization

Extraction of polyethylene chain from the HDPE-g-YDH151/BT and HDPE/BT composites was carried out using xylene in a Soxhlet extractor at 140 °C for 48 h, then filtered and dried in a vacuum oven at 80 °C for 12 h. Whereafter these samples were extracted again by chloroform

at 80 °C for 24 h to extract the unreacted vinyl triethoxysilane, and then filtered and dried in a vacuum oven at 60 °C. At last, these samples were characterized by FT-IR.

Results and discussion

The reaction between HDPE-g-YDH151 and BT

HDPE-g-YDH151/BT composites were prepared via melt compounding in ThermoHaake Rheomix. Fig. 1 shows the torque versus time for the composites during compounding process. It is found that the torque is primarily unchanged with adding 2phr and 4phr BT into primal HDPE directly. HDPE/DCP has a second maximal peak which is correspondent to the crosslinking of HDPE induced by DCP. Such a second maximal peak is much more significant in HDPE/DCP/YDH151 system, inferring that YDH151 improves the crosslinking reaction. While adding BT into HDPE/DCP/YDH151, the second maximal torque and the equilibrium torque decrease, moreover the more BT added the lower the torque is. It indicates that BT prohibits the crosslinking reaction.

Fig. 2 shows the FT-IR spectra of HDPE and HDPE-g-YDH151. It is found that new peaks appear at 1070 cm^{-1} when compared to the pure HDPE, indicating that YDH151 has been successfully grafted onto polyethylene chain.

HDPE-g-YDH151 chain has hydroxyl groups which can react with the amidogens. It is confirmed by FT-IR spectra (Fig. 3). In Fig. 3, *a* is the curve of pure BT, 1042.1 cm^{-1} is the characteristic peak of octadyl trimethyl ammonium; *b* and *c* are the curves of HDPE/BT (*b*) and HDPE-g-YDH151/BT (*c*) after extracted with xylene and chloroform. Comparing *a* with *b*, we can find that the two curves are same, indicating that the extracted residue of HDPE/BT is only BT, and the polyethylene has been totally extracted. The result infers that the chain of polyethylene did not bond with BT. In comparison, the change in curve *c* is evident: first, the intensity of amine peak reduced, revealing that part of amine reacted with hydroxyls of YDH151; second, there is a characteristic peak of polyethylene at 1470.6 cm^{-1}; third, there is a strong peak of hydroxyl at 3435.3 cm^{-1}. These results indicate that HDPE-g-YDH151 has been chemically bonded with BT.

The dispersion of C18-BT in HDPE and HDPE-g-YDH151

The direct evidence of the intercalation is provided by the XRD patterns of the obtained hybrids. The XRD spectrum of the organoBT exhibits a broad intense peak at around 4.2°, corresponding to a basal spacing of 2.09 nm. The XRD pattern of the mixture of BT (2phr, 4phr) with HDPE is presented in Fig. 4. The result clearly shows that the (001) plane peak of the clay does not change and polyethylene chains do not intercalate into BT. It is because that polyethylene does not include any polar group in its backbone, and the silicate layer of clay, even modified by non-polar long alkyl groups, are polar and incompatible with polyolefin.

Fig. 4 also shows the XRD patterns of HDPE-g-YDH151 compounding with the same content of BT. Comparing to these curves, the peaks of BT around $2\theta = 4.2$ are shifted to lower angles, revealing the intercalation of HDPE or/and HDPE-g-YDH between the silicate layers. This result indicates that the modification of YDH151 grafting promotes the penetration of PE chains into layered BT.

In order to confirm the dispersion of BT in HDPE-g-YDH151 and pure HDPE, TEM was used to directly view the structure of nanocomposites (Fig. 5). Obviously, the dispersion of BT was much better in HDPE-g-YDH151/BT composites (E–H) than in HDPE/BT composites (A–D). Some of the BT has exfoliated into single sheets in HDPE-g-YDH151/BT composites. While in HDPE/BT composites, BT aggregates are not intercalated by PE chains. It is realized that polyethylene nanocomposite with good exfoliation or intercalation can be obtained by proper modification of HDPE.

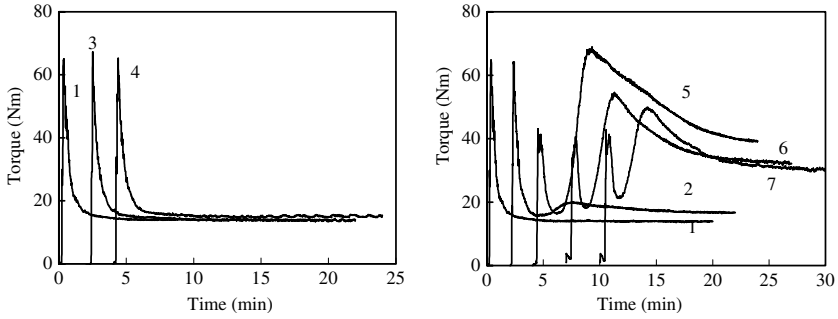

Fig. 1 The change of torque with increasing the time during the melt compounding of HDPE-g-YDH/BT and HDPE/BT system: (1) pure HDPE; (2) HDPE/DCP(100/0.1); (3) HDPE/MMT(100/2); (4) HDPE/MMT(100/4); 5–7: HDPE/YDH-151/DCP/MMT(100/8/0.1/*x*) the content of MMT as follows: 5(0phr); 6(2phr); 7(4phr)

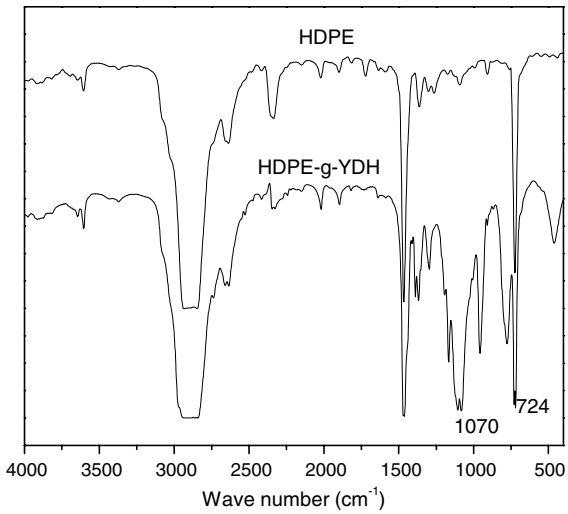

Fig. 2 FT-IR spectra of HDPE and HDPE-g-YDH151, the unreacted YDH151 has been extracted with chloroform

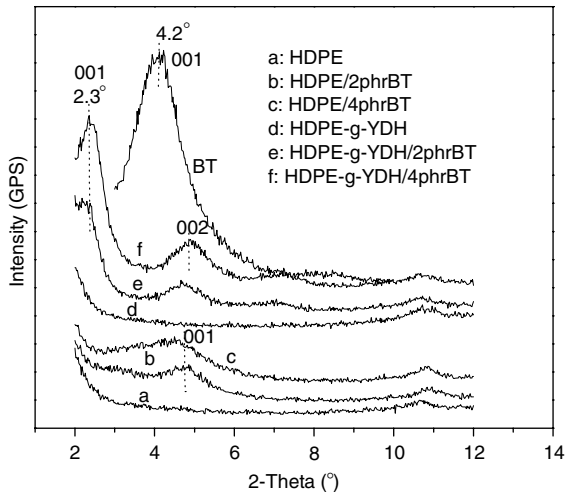

Fig. 4 XRD patterns of BT, HDPE/BT and HDPE-g-YDH/BT

Mechanical properties

Table 1 lists the tensile strength, elongation at break, and Young's modulus for HDPE, HDPE-g-YDH151 and their BT composites. As shown in Table 1, the tensile strength and Young's modulus of HDPE-g-YDH151 are lower than that of HDPE, while elongation at break is higher than that of HDPE. It's because that crosslinking and grafting reaction of HDPE reduced average molecular weight of HDPE, leading to the decrement of strength and modulus. While because of the increment of polarity of HDPE chain, elongation at break increased.

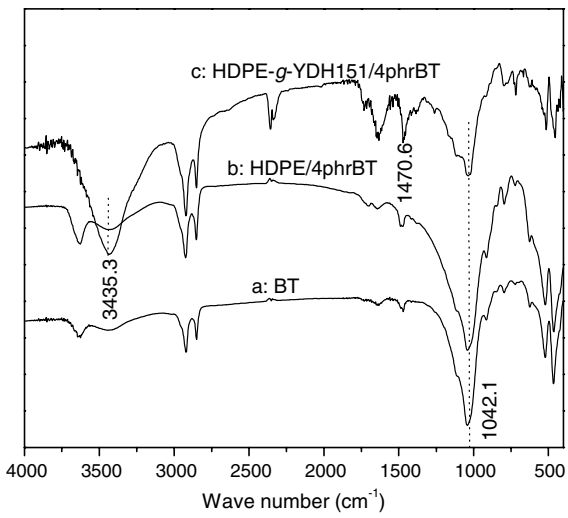

Fig. 3 FT-IR spectra of BT and the drawers of HDPE-g-YDH/4phr BT and HDPE/4phr BT

When adding the 2phr and 4phr BT to HDPE, we found that almost all mechanical properties decreased compared with primal HDPE, only the addition of 4phr BT increased Young's modulus to 451.7 MPa. It is because that BT cannot disperse well in HDPE matrix or sometimes gathered, that will lead to cavity in matrix. This suggestion can be corroborated based on SEM observation of side surface of the tensile specimens near the fracture site (Fig. 6). Picture A–D shows the side surface of the tensile specimens near the fracture site of HDPE/BT composites, the elongated voids are large and slick and the interfacial adhesion between the filler and the matrix is very week. Moreover, when adding 4phr BT into HDPE matrix, the length of elongated void is more than 1000 μm.

In comparison, adding 2phr BT into HDPE-g-YDH (picture E), the size of elongated voids distinctly decreases and there are strong interfacial adhesion between the filler and the matrix, so its mechanical properties are good, the elongation at break improved 29% and Young's modulus increased 32%. When adding 4phr BT (picture F), the size of elongated voids increases and the mechanical properties decreased.

Thermal behavior of composites

Figure 7 and Table 1 displays the melting temperature (T_m) and melting endotherms (ΔH) of polyethylene in HDPE-g-YDH151/BT and HDPE/BT composites, respectively. As shown in Table 1, T_m and ΔH of HDPE-g-YDH151 are lower than that of HDPE. It is because that crosslinking and grafting reaction of HDPE reduces the mobility of crystallizable HDPE chain segments. However, because of the increment of polarity of HDPE-g-YDH151, T_m decreased.

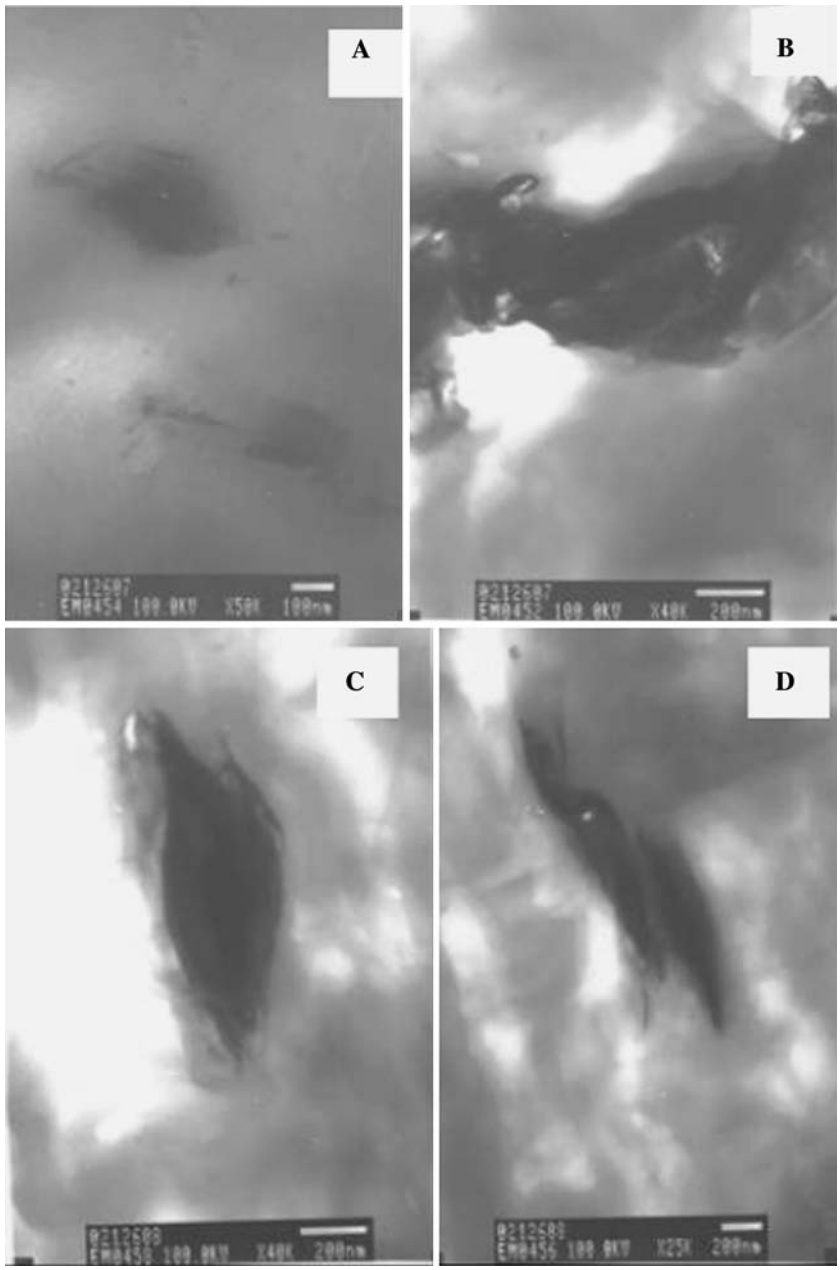

Fig. 5 TEM observations for HDPE-g-YDH151/BT and HDPE/BT: **a** and **b**: HDPE/2phrBT; **c** and **d**: HDPE/4phrBT; **e** and **f**: HDPE-g-YDH151/2phrBT; **g** and **h**: HDPE-g-YDH151/4phrBT

When adding 2phr and 4phr BT into HDPE and HDPE-g-YDH151, we found that the peak melting temperature and ΔH of HDPE-g-YDH151/BT composites are slightly higher than that of HDPE-g-YDH151 while lower than that of HDPE. These changes may be attributed to high interfacial adhesion between the HDPE-g-YDH151 matrix and exfoliated clay, which reduces the mobility of crystallizable PE chain segments, and subsequently reduces the crystallization ability.

In comparison, when we add 2phr, 4phr BT to HDPE, we find that melting temperature and melting endotherms nearly unchanged, inferring weak interaction between HDPE matrix and BT.

Conclusions

Chemical modification of both the polyethylene and BT clay is necessary to generate polyethylene/BT nanocomposites by melt compounding. XRD and TEM results indicate that YDH151 promotes the dispersion and exfoliation of BT into HDPE. Most of the BT has exfoliated into single sheets in HDPE-g-YDH151/BT composites. While in HDPE/BT composites, most of the BT aggregates are not intercalated by PE chains. Consequently, the mechanical properties of HDPE-g-YDH151/BT are good, while that of HDPE/BT composites is poor. Moreover, because of the high interfacial adhesion between

Fig. 5 continued

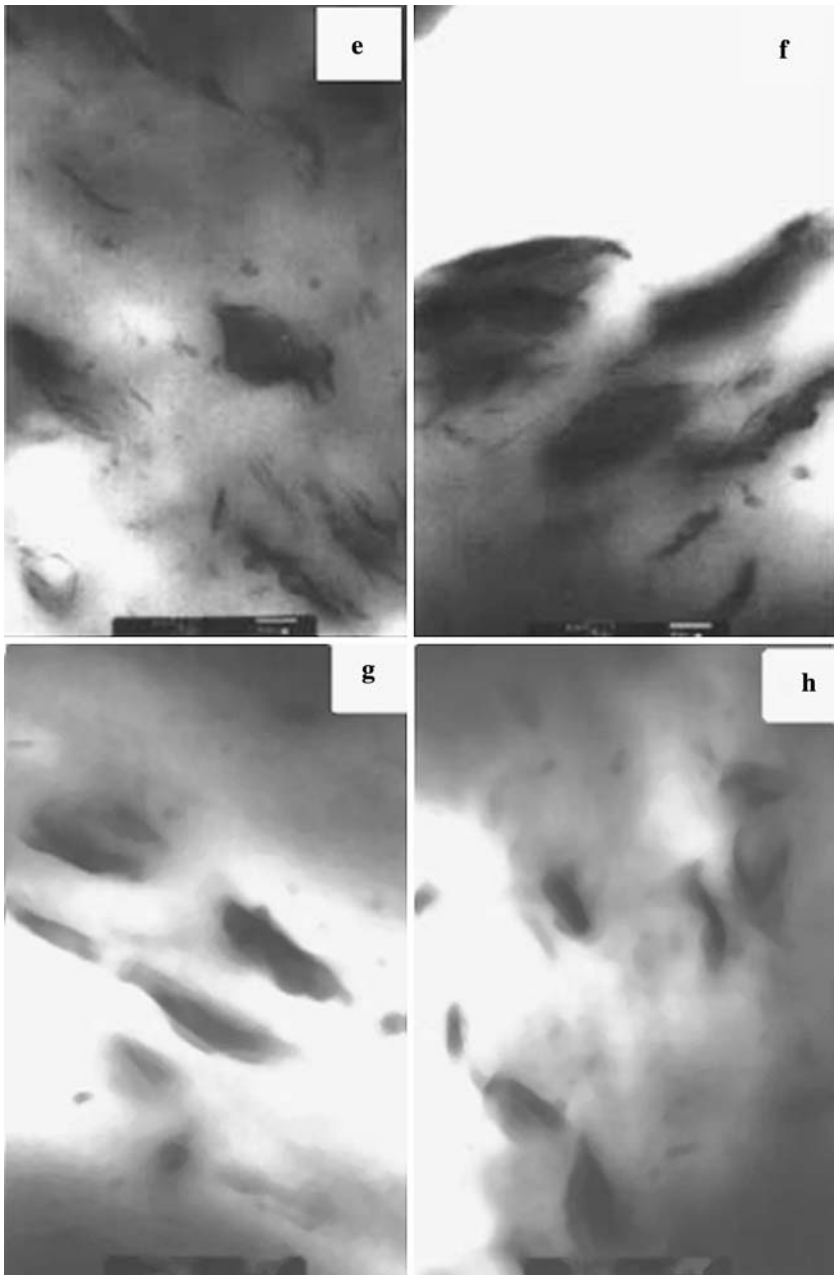

Table 1 Mechanical and thermal properties of HDPE, HDPE-g-YDH and their composites with BT

Samples	HDPE/BT			HDPE-g-YDH/BT		
BT content (phr)	0	2	4	0	2	4
Tensile strength (MPa)	29.0	28.7	27.1	24.4	25.3	24.3
Elongation at break (%)	360.7	127.4	177	388.0	500.8	235.7
Young's modulus (MPa)	397.7	392.7	451.7	353.2	466.7	367.7
Melting temperature (°C)	134.2	134.0	133.7	128.5	130.0	128.8
Melting endotherms (J/g)	205.5	204.9	204.8	163.6	175.2	164.7

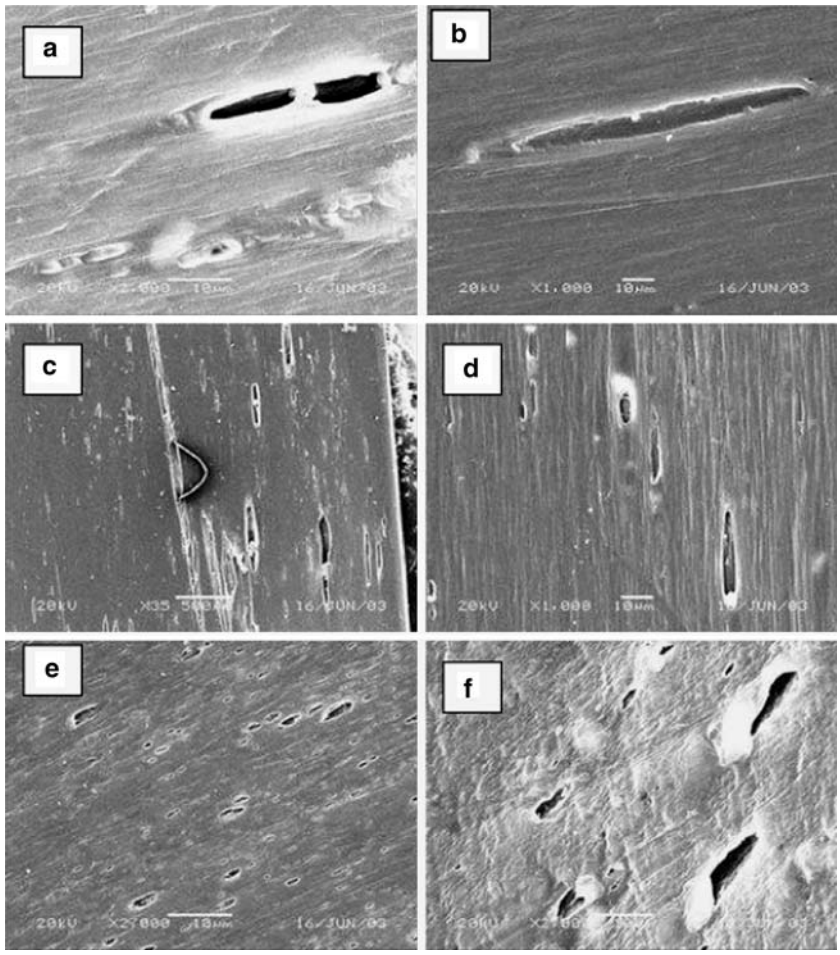

Fig. 6 SEM observations for the side surface of the tensile specimens near the fracture site of HDPE-g-YDH151/BT and HDPE/BT: **a** and **b**: HDPE/2phrBT; **c** and **d**: HDPE/4phrBT; **e**: HDPE-g-YDH151/2phrBT; f: HDPE-g-YDH151/4phrBT

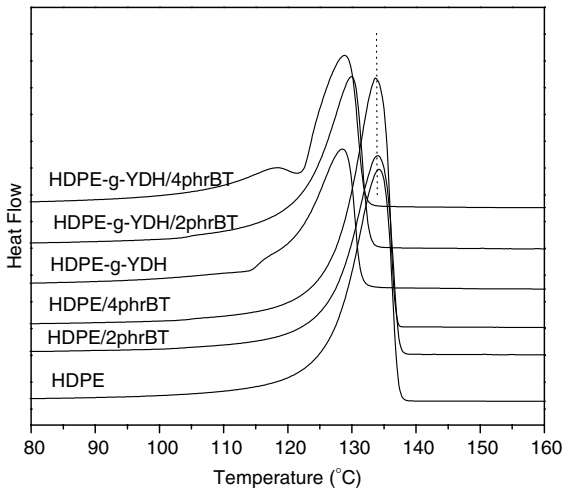

Fig. 7 DSC curves of HDPE, HDPE-g-YDH151 and their composites with BT

HDPE-g-YDH151 matrix and exfoliated BT, the mobility of crystallizable PE chain segments as well as their crystallization ability are reduced. In comparison, the addition of BT to HDPE does not affect the crystallization behavior of the later.

References

1. Kojima Y, Usuki A, Kawasumi M, Okada A, Fukushima Y, Kurauchi T, Kamigaito O (1993) J Mater Res 8:1185
2. Kojima Y, Usuki A, Kawasumi M, Okada A, Kurauchi T, Kamigaito O (1993) J Appl Polym Sci 49:1259
3. Kawasumi M, Hasegawa N, Kato M, Usuki A, Okada A (1997) Macromolecules 30:6333
4. Vaia RA, Vasudevan S, Krawiec W, Scanlon SG, Giannelis EP (1995) Adv Mater 7:154
5. Giannelis EP (1996) Adv Mater 8:29
6. Choi MH, Chung IJ, Lee JD (2000) Chem Mater 12:2977
7. Wang KH, Choi MH, Koo CM, Chung IJ (2001) Polymer 42:9819
8. Lebaron PC, Wang Z, Pinnavaia T (1999) J Appl Clay Sci 15:11
9. Alexandre M, Dubois P (2000) Mater Sci Eng 28:1
10. Onsager L, Ann NY (1949) Acad Sci 51:627
11. Langmuir I (1938) J Chem Phys 6:873
12. Davidson P, Batail P, Gabriel JCP, Livage J, Sanchez C, Bourgaux C (1997) Prog Polym Sci 22:913
13. Gabriel JCP, Davidson P (2000) Adv Mater 12:9
14. Gabriel JCP, Sanchez C, Davidson P (1996) J Phys Chem 100:11139
15. Van der Kooij FM, Kassapidou K, Lekkerkerker HNW (2000) Nature 406:868
16. Lekkerkerker HNW, Stroobants A (1998) Nature 393:305
17. Lyatskaya Y, Balazs AC (1999) Macromolecules 31:6676

18. Balazs AC, Singh C, Zhulina E, Lyatskaya Y (1999) Acc Chem Res 32:651
19. Ginzburg VV, Balazs AC (1999) Macromolecules 32:5681
20. Ginzburg VV, Singh C, Balazs AC (2000) Macromolecules 33:1089
21. Ginzburg VV, Balazs AC (2000) Adv Mater 12:1805
22. Vaia RA, Jandt KD, Kramer EJ, Giannelis EP (1995) Macromolecules 28:8080
23. Hackett E, Manias E, Giannelis EP (2000) Chem Mater 12:2161
24. Bujdak J, Hackett E, Giannelis EP (2000) Chem Mater 12:2168
25. Vaia RA, Sauger BB, Tse OK, Giannelis EP (1997) J Polym Sci Part B: Phys 35:59
26. Krishnamoorti R, Vaia RA, Giannelis EP (1996) Chem Mater 8:1728
27. Krishnamoorti R, Vaia RA, Giannelis EP (1997) Macromolecules 30:4097
28. Vaia RA, Giannelis EP (1997) Macromolecules 30:8000
29. Lim YT, Park OO (2000) Macromol Rapid Commun 21:231
30. Lim YT, Park OO (2001) Rheol Acta 40:220
31. Jeon HG, Jung HTS, Lee W, Hudson SD (1998) Polym Bull 41:107
32. Furuichi N, Kurokawa Y, Fujita K, Oya A, Yasuda H, Kiso M (1996) J Mater Sci 31:4307
33. Heinemann J, Keichert P, Thomann R, Mulhaupt R (1999) Macromol Rapid Commun 20:423
34. Alexandre M, Dubois P, et al. WO9947598A1
35. Bergman JS, Chen H, Giannelis EP, Thomas MG, Coates GW (1999) Chem Commun 2179
36. Hudson SD US5910523A
37. Inoue H, Hosokawa T EP 0807659A1
38. Kurokawa Y, Yasuda H, Oya A (1996) J Mater Sci Lett 15:1481
39. Kurokawa Y, Yasuda H, Oya A (1997) J Mater Sci Lett 16:1670
40. Oya A, Kurokawa Y, Yasuda H (2000) J Mater Sci 35:1045
41. Usuki A, Kato M, Okada A, Kuraushi T (1997) J Appl Polym Sci 63:137
42. Kato M, Usuki A, Okada A (1997) J Appl Polym Sci 66:1781
43. Kawasumi M, Hasegawa N, Kato M, Usuki A, Okada A (1997) Macromolecules 30:6333
44. Hasegawa N, Kawasumi M, Kato M, Usuki A, Okada A (1998) J Appl Polym Sci 67:87